BIG – Branschsamverkan i grunden

Forskningsprogram för effektiv och säker grundläggning av vägar och järnvägar

Projekt A2018:03

Three-dimensional effects in slope stability calculations

Final report from project

KTH
CHALMERS UNIVERSITY OF TECHNOLOGY
TRAFIKVERKET
STATENS GEOTEKNISKA INSTITUT
LULEÅ TEKNISKA UNIVERSITET

BIG – Branschsamverkan i grunden
Forskningsprogram för effektiv och säker grundläggning av vägar och järnvägar

Rapport BIG projekt A2018:03

Three-dimensional effects in slope stability calculations

Final report from project

LULEÅ TEKNISKA UNIVERSITET

Framtagen inom ramen för BIG av Luleå tekniska universitet

Luleå 2021

Rapport publicerad av BIG, Branschsamverkan i grunden
Beställning Web: www.big-geo.se

ISBN 978-91-986926-6-2
Upplaga Digital

Framtagen av Luleå tekniska universitet
Department of Civil, Environmental and Natural Resources Engineering
Författare Jingjing Meng, Hans Mattsson, Jan Laue

Three-dimensional effects in slope stability calculations

Jingjing Meng, Hans Mattsson, Jan Laue

Department of Civil, Environmental and Natural Resources Engineering,
Luleå University of Technology, Sweden

Preface

The work presented in this report has been financially supported by Swedish Transportation Administration research program BIG (Branschsamverkan I Grunden). The project number is A2018-03. We gratefully acknowledge the financial support that makes this study happen.

We thank the helpful discussion from the reference group: Dr. Kenneth Viking and Mr. Niklas Dannewitz at Swedish Transportation Administration (Trafikverket), and Prof. Göran Sällfors and Prof. Minna Karstunen at Chalmers University of Technology.

Sammanfattning

Två-dimensionella (2D) metoder baserade på gränslastteori används vanligtvis för släntstabilitets-analys. Den två-dimensionella förenklingen ger normalt säkerhetsfaktorer med värden som är lägre än säkerhetsfaktorerna för den verkliga tre-dimensionella (3D) slänten. Anledningen är att hållfasthet i den tredje dimensionen inte inkluderas vid två-dimensionella släntstabilitetsanalyser. Stora ekonomiska resurser används varje år till att förstärka slänter för att erhålla en tillräcklig säkerhet mot skred baserat på två-dimensionella analyser. En del av dessa kostnader kan sparas om tre-dimensionella effekter beaktas vid släntstabilitetsanalys. Av den anledningen blir det viktigt att uppskatta hur tre-dimensionella effekter påverkar stabiliteten för olika typer av slänter. Om de tre-dimensionella effekterna är betydande rekommenderas att en detaljerad tre-dimensionell slänt-stabilitetsanalys genomförs, annars kan det vara tillräckligt med en enklare två-dimensionell analys.

Ett mått på 3D-effekternas betydelse för en släntstabilitetsanalys är hur värdena på säkerhets-faktorerna vid 3D-analys (FS3D) och 2D-analys (FS2D) särskiljer sig. I denna studie beräknas 3D-effekterna med kvoten FS3D/FS2D. En serie av FS3D/FS2D grafer har framtagits för homogena slänter med olika geometri och hållfasthet. Finita elementprogrammet PLAXIS och gränslastanalys-programmet SLOPE/W har använts vid beräkning av säkerhetsfaktorer. För en idealiserad slänt under odränerade förhållanden har FS3D/FS2D grafer upprättats där släntens lutning, bredd, krönhöjd och djup till fast botten varieras. På motsvarande sätt har FS3D/FS2D grafer upprättats för en idealiserad slänt under dränerade förhållanden. Släntens lutning, bredd, krönhöjd och hållfasthetsparametervärden varieras. Dessutom har FS3D/FS2D grafer tagits fram för en konkav slänt under dränerade förhållanden. Släntens lutning, radie i horisontalplanet, krönhöjd och hållfast-hetsparametervärden varieras. De framtagna graferna i denna studie kan användas för att avgöra huruvida tre-dimensionella effekter bör beaktas vid släntstabilitetsanalys. Slänten måste naturligtvis ha en geometri som överensstämmer med den här studerade. En två-dimensionell analys är tillräcklig om kvoten FS3D/FS2D ligger nära ett, annars bör en detaljerad tre-dimensionell analys genomföras. Graferna kan även användas till att studera hur 3D-effekterna påverkas när storheterna i graferna varieras.

Ett datorprogram SlopeLab har utvecklats, i detta projekt, utgående från FS3D/FS2D graferna samt ett matematiskt verktyg baserat på artificiella neurala nätverk. Efter att släntens geometri och hållfasthet angetts som indata till SlopeLab erhålls kvoten FS3D/FS2D direkt. Även FS3D och

FS2D ges för den idealiserade slänten som en preliminär uppskattning. För att kontrollera tillförlitligheten hos programmet SlopeLab har en grupp släntstabilitetsexempel analyserats med programmet. Det visade sig att SlopeLab kan bestämma säkerhetsfaktorers värden med en stor noggrannhet för idealiserade slänter.

Abstract

Two-dimensional (2D) limit equilibrium methods are still commonly used for slope stability analysis. However, the factor of safety based on 2D analysis can be much lower than the real factor of safety of a slope in three-dimensional (3D) space. The reason is that boundary restrictions in the third dimension are not included in 2D slope stability analyses. A large amount of money needs to be spent on improving the stability of slopes to meet a certain safety factor requirement according to 2D calculate results every year. However, a considerable percentage of the spending can be avoided if the improvement of the factor of safety by 3D effects to can be considered. Therefore, it is important to estimate the three-dimensional (3D) effect in slope stability analyses. When the 3D effect is significant, a detailed 3D slope stability analysis that can consider complex 3D geometry and boundary condition is advised.

The 3D effect measures the difference between the three-dimensional factor of safety (*FS3D*) and the two-dimensional factor of safety (*FS2D*). It is calculated with *FS3D*/*FS2D* in this work. A finite element program, Plaxis and a limit equilibrium code SLOPE/W are used in this study for slope stability analyses. The 10-node tetrahedral elements with a second-order interpolation of displacements are chosen in Plaxis 3D. Default convergence parameters with respect to solving *FS* in Plaxis 3D and SLOPE/W are used. A series of charts on 3D effects are presented for slopes under different conditions. For purely cohesive slopes, a slope geometry model is used with parameters including the slope height, the slope width, the slope angle and the slope depth. The shear strength of the soils is defined with undrained shear strength. For cohesive-frictional soil slopes, the shear strength of the soils is defined with cohesion and internal frictional angle. A wide range of slope parameters are considered for the charts and the slope angle is increased from 15˚ to 90˚ with an interval of 15˚. In addition to the straight slopes, the three-dimensional stability assessment of concave slopes is conducted. A radius is used to define the slope surface' curvature in the horizontal plane. The cohesive-frictional soil shear strength is considered and associated 3D effect charts are proposed. Given a slope, a fast estimation of the 3D effect can be performed with the charts. When the 3D effect is small, it is understandable that 2D analyses for the slope stability are justifiable. If not, a detailed 3D slope stability analysis that can consider complex 3D geometry and boundary condition is advised. In addition, engineers can also understand the impact of slope parameters on 3D effects from the charts.

A computer program, SlopeLab is developed based on the data in the charts and a mathematical model, artificial neural networks. After setting the slope parameters in the program, the 3D effect, *FS3D*/*FS2D*, can be obtained from the program immediately. In addition, *FS3D* and *FS2D* can also be obtained for the idealised slopes, which are merely to provide a preliminary estimation. A series of numerical examples have been used to test the program. The results show that SlopeLab can predict the stability of slopes with a great accuracy.

Table of contents

Preface I

Sammanfattning II

Abstract IV

Table of contents VI

1. Introduction 1

2. Three-dimensional effects 4

3. Charts of three-dimensional effects 10

3.1 Purely cohesive slopes 10

3.2 Cohesive-frictional soil slopes 12

3.3 Concave slopes 13

4. An easy-to-use tool: SlopeLab 17

5. Application examples 19

5.1. Example 1: an undrained slope 19

5.2. Example 2: a cohesive-frictional soil slope 21

5.3. Example 3: a concave slope 23

Conclusions and discussions 24

References 26

1. Introduction

Slope stability analysis is a common task in geotechnical engineering due to its essential role in maintaining the stability of natural slopes and designing man-made structures such as railway embankments, dams and highways etc. The stability of slopes is quantified in the form of the factor of safety (*FS*). In order to simplify the process of calculating *FS*, a vast majority of slope stability analyses in engineering practice are performed in two-dimensions (2D) under plane strain assumption, in which the slope is infinitely wide such that three-dimensional (3D) end effects are negligible. However, numerous studies have been performed showing that two-dimensional slope stability analysis presents a lower *FS* than the real factor of safety of a slope in 3D (Leshchinsky and Baker, 1986, Zhang et al., 2015, Park and Michalowski, 2017, Zhang et al., 2018). In the literature (Li et al., 2009b, Zhang et al., 2015, Lim et al., 2016), differences between the two-dimensional factor of safety (*FS2D*) and three-dimensional factor of safety (*FS3D*) are found greater than 50% for some slopes. Therefore, the prediction based on 2D analysis can be very inaccurate.

With increasing computational power and availability of 3D analysis methods, it should be more acceptable to consider also 3D effects especially if the boundary conditions of the long slopes are not given or if local construction needs to be considered. The cost of slope engineering can be reduced significantly through the application of 3D slope stability analysis because 3D slope stability analyses can provide a higher and more accurate factor of safety.

For 2D analyses, Limit Equilibrium Method (LEM) is developed well in terms of both theory and engineering practice. However, the developments of 3D limit equilibrium methods are lacking. Jiang and Zhou (2017) proposed a rigorous limit equilibrium method for 3D asymmetrical slope stability analysis. Global equilibrium equations are formulated in light of the safety factor, sliding direction, and an assumed distribution of normal stress on the slip surface. In the literature (Lu and Zhu, 2016), the function of the normal stress over the slip surface is simulated with five unknowns. In the paper (Cheng and Zhou, 2015), a novel displacement-based rigorous limit equilibrium method is proposed to investigate the displacements and stabilities of three-dimensional landslides. Introducing the Morgenstern–Price assumption on the internal forces of the slip body, the 3D Morgenstern–Price method that is rigorous and applicable to failure surfaces of complex shape is proposed (Zheng, 2012).

(Dong-ping et al., 2017) proposed 3D limit equilibrium methods with general-shaped slip surfaces. In addition, limit equilibrium methods have been improved with optimization algorithms recently (Pandit et al., 2019). In order to determine the 3D shape of failure in soil slopes, particle swarm optimization in a 3D LEM is proposed based on a new equation to calculate the direction of sliding and *FS* (Kalatehjari et al., 2015).

In contrast to LEM, the failure mechanism at the critical equilibrium state can be obtained automatically from calculation results by advanced numerical methods such as the Finite Element Method (FEM) (Leroueil, 2001). The failure mechanism is resolved from simulation results so the failure assumption is not required in the calculation. Thus, it has become a standard slope stability method throughout the literature (Griffiths and Marquez, 2007, Hicks and Li, 2018). Tension cut-off is introduced into the Mohr-Coulomb yield condition for 3D slope stability (Park and Michalowski, 2017). Hoek–Brown (HB) criterion is introduced to analyse 3D slope stability using the shear strength reduction technique (Shen and Karakus, 2013). The finite element approach with an elasto-viscoplastic strain-softening model has been employed in (Troncone et al., 2014).

Limit Analysis (LA) is another method that can be used for 3D slope stability analyses, and both analytical and numerical strategies are available (Drescher and Michalowski, 2009, Michalowski, 2010, Sloan, 2013). Its accuracy and powerful performance have been demonstrated in analysing the stability of various slopes, such as the seismic rock slope (Li et al., 2009a), the two-layered cohesive soil slope (Qian et al., 2015) and the slope with cracks (Utili, 2013). Analyses of three-dimensional slope failures were conducted using admissible kinematics of limit analysis (Park and Michalowski, 2018). *FS* calculated by the strength reduction method and the gravity increase method is compared in (Yang and Li, 2018).

Slope stability charts have been used in practice as a preliminary analysis tool to estimate *FS* for a slope before personal computers are widely available (Taylor, 1937, Bishop and Morgenstern, 1960, Bell, 1966). While computational methods have made most stability charts obsolete, dimensionless slope parameters are formulated with a clear relationship in the charts. Since more results on *FS* of slopes under different conditions are available (Gao et al., 2013, Qian et al., 2015, Sun et al., 2017), the charts have been developed further. They serve a good purpose of preliminary and back analyses.

In this work, 3D effects in slope stability analyses are investigated and measured with a ratio of the safety factor, *FS3D*/*FS2D*. A 3D finite element software, Plaxis 3D with strength reduction method (Brinkgreve et al., 2010) is used for 3D slope stability analyses. The 10-node tetrahedral elements with a second-order interpolation of displacements are chosen in Plaxis 3D. Over 50 000 elements are used in the numerical models normally. The default numerical iteration parameters in Plaxis are adopted.

A conventional 2D slope stability analysis is performed using the limit equilibrium method (Bishop) with the computer program, SLOPE/W (Krahn, 2004). At least 30 slices are used in limit equilibrium analyses. The convergence parameters are set as: the maximum number of iterations=100 and the *FS* tolerance =0.001. Data from stability charts have been collected and examined. A series of charts on 3D effects are presented for slopes under different conditions. For purely cohesive slopes, a slope geometry model is used with parameters including the slope height, the slope width, the slope angle and the slope depth. The shear strength of the soils is defined with undrained shear strength. For cohesive-frictional soil slopes, the shear strength of the soils is defined with cohesion and internal frictional angle. A wide range of slope parameters are considered for the charts. In addition to the straight slopes, the three-dimensional stability assessment of concave slopes in plan view is conducted. The cohesive-frictional soil shear strength is considered and associated 3D effect charts are proposed. A most relevant case can be found in the charts so a preliminary estimation on 3D effects can be done. Furthermore, based on available data, an artificial neural network is trained to develop a digital tool, SlopeLab for ease of use. A series of examples will be employed to demonstrate how it can be used. The results can help practical engineers to decide whether 3D effects of a slope are significant. When the value of the variable, *FS3D*/*FS2D* is large (such as larger than 1.2), a detailed 3D slope stability analysis that can consider complex 3D geometry and boundary condition is advised

2. Three-dimensional effects

To compare the slope stability analysis methods and show 3D effects, our study begins with an idealised slope as shown in Fig.1:

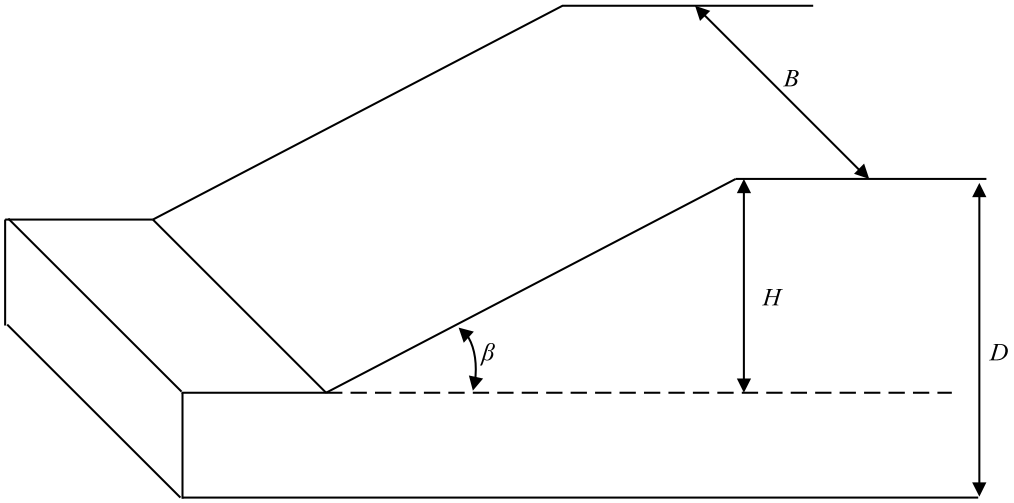


Fig. 1 The geometric model of the slope.

In the first example, the slope parameters are cohesive strength c=5 kPa, internal frictional angle ϕ=20˚, slope height H=4.5 m and slope depth D=6.5 m. To study the 3D effects, slope width B is increased from 1 m, 2 m, 4.5 m, 9 m, 18 m, 36 m and 72 m. In addition, the impact of the load is considered with an external load of 30 kPa imposed on the slope crest and the load width on the slope crest is 3 m, as shown in Fig. 2 (b). The 2D slope stability analysis results by the limit equilibrium method, Bishop and the strength reduction method by Plaxis 3D are compared in Fig. 2. The results show a very good agreement regarding both *FS* and the position of the failure surface.

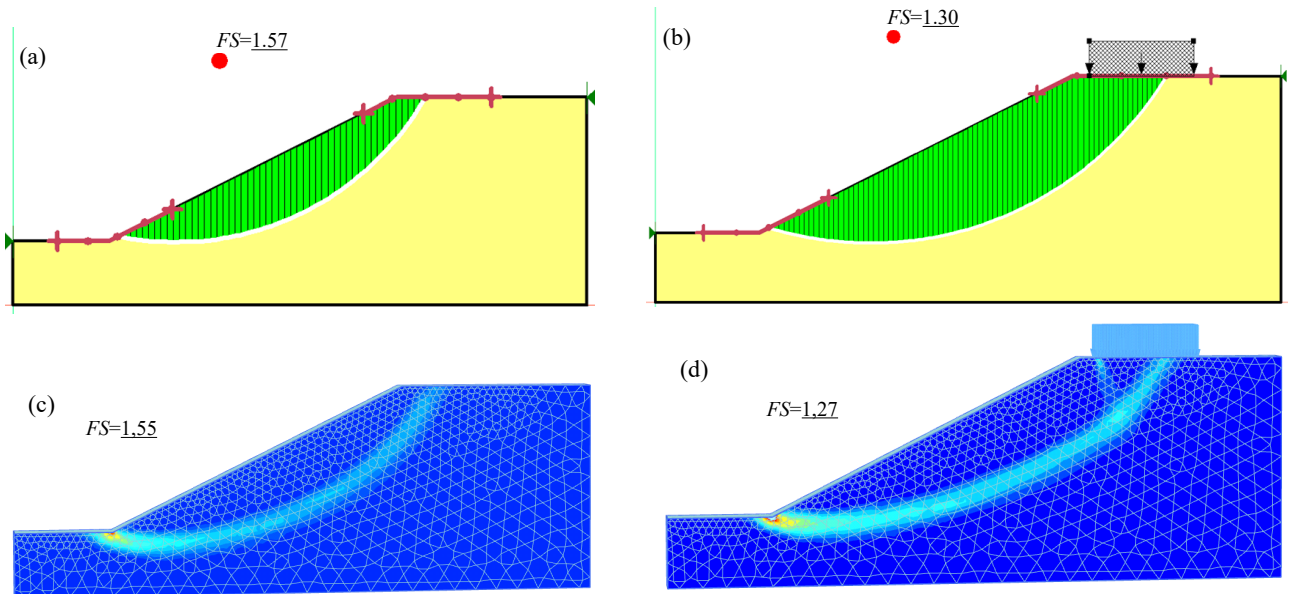


Fig. 2. 2D numerical results for the slope: (a) limit equilibrium analysis, (b) limit equilibrium analysis for a slope, (c) strength reduction method and (d) strength reduction method with a load. For finite element numerical results, colours are proportional to the total deviatoric strain.

Following the standard strength reduction procedures in Plaxis, the factor of safety of slopes can be determined from the finite element numerical results. Fig. 3 shows results on reduction factors against nodal displacement of the crest of slope model. As the soil strength is gradually reduced, the displacement is increased. The critical reduction factor (i.e., the factor of safety) is determined until the displacement witnesses a subsequent significant increase, which is a classic slope failure criterion. In Fig.3, slope failure is indicated with dashed lines.

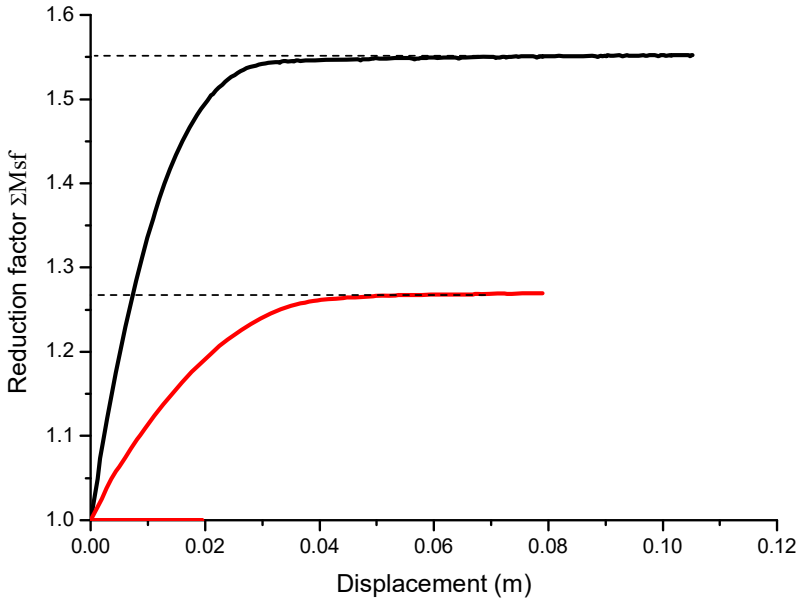


Fig. 3 Reduction factors against the nodal displacement on the slope crest. Black and red lines represent the slope without and with the external load.

To study the 3D effects, 3D slope stability analyses are performed with the strength reduction method by Plaxis 3D. The ‘rough- rough’ boundary condition is set as follows: two end faces in the third dimensions are fully fixed (rough); the bottom is fully fixed and the slope surface is free to move. This boundary is assumed when failure zone is far inside the region. For more information, interested readers can refer to the references (Chugh, 2003, Griffiths and Marquez, 2007). The numerical results regarding the failure surface are shown in Fig. 4. In contrast to the 2D analysis, the shapes of the failure surfaces are changed in the third dimension. The slopes’ end faces are constrained, providing additional supports to the stability of the slopes.

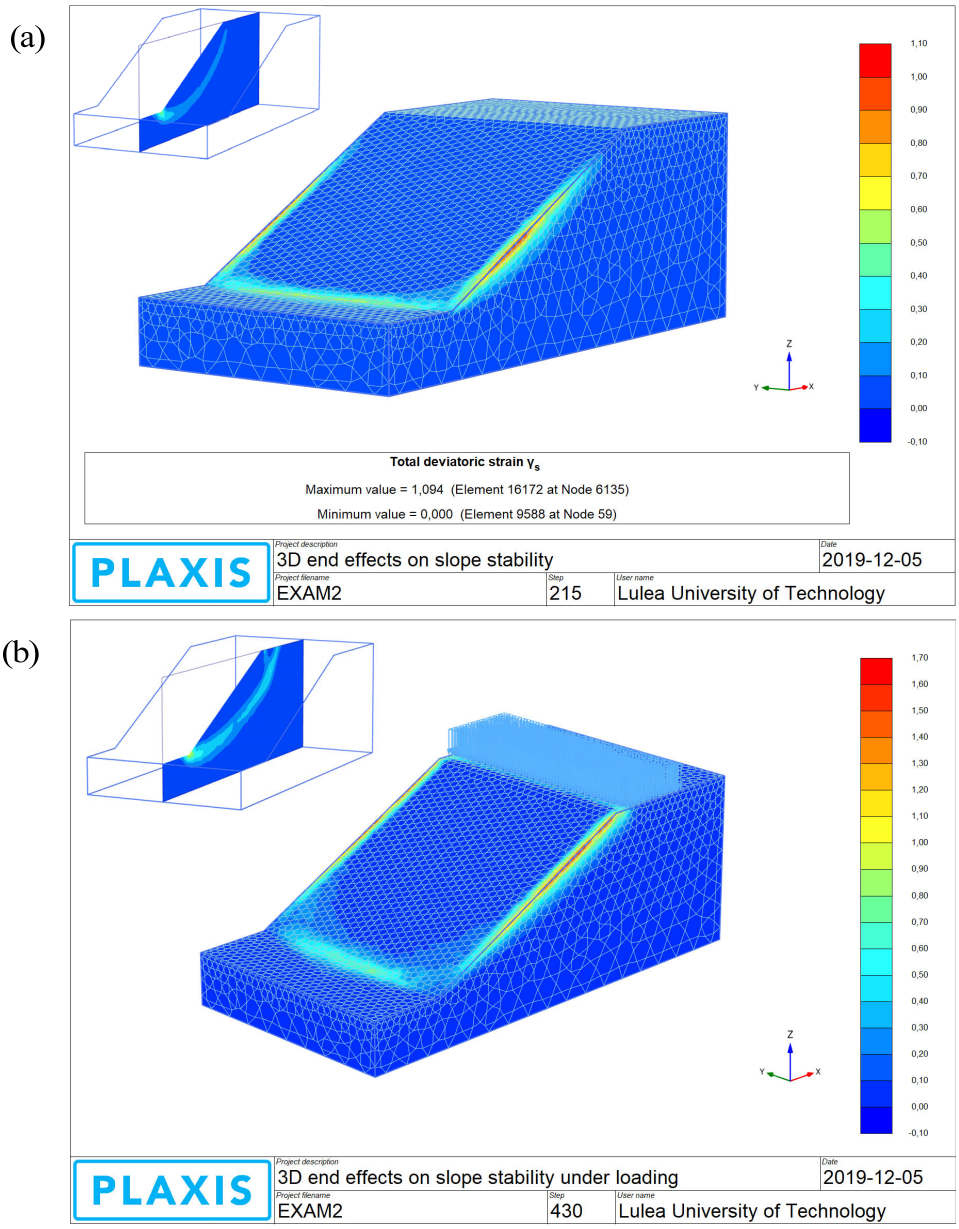


Fig. 4. 3D failure surface of a slope: (a) without loads and (b) with loads. Colours are proportional to the total deviatoric strain.

Regarding *FS*, a comparison of the 2D and 3D slope stability analysis is given in Fig. 5. It is evident that *FS3D* is higher than *FS2D* and the difference is getting smaller with B/H increases. According to the figure, the 2D solution is acceptable for the slope when $B/H \geq 4$ as the 3D effect is insignificant ($FS3D/FS2D < 1.1$).

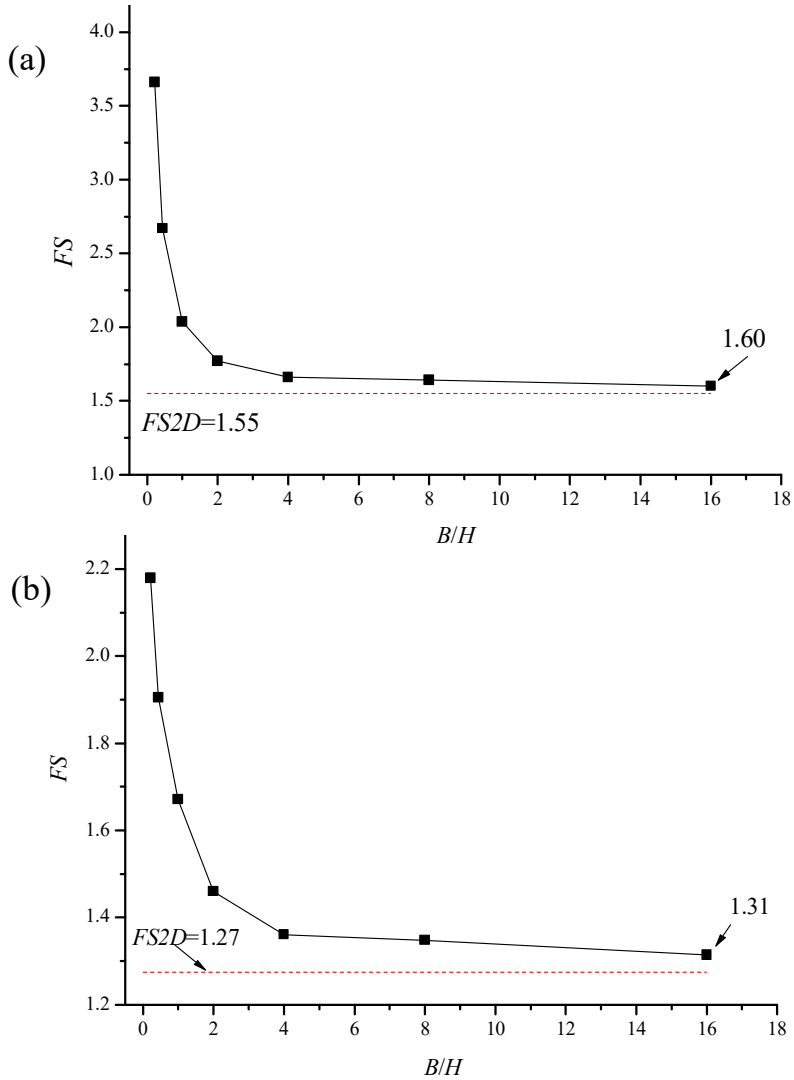


Fig. 5. *FS3D* for slopes with varied *B*/*H*: (a) without the load and (b) with the distributed load on slope crest.

To investigate the effect of mesh quality on numerical results, mesh sensitivity analysis is conducted. A typical three-dimensional slope with *B/H*=2 is used and discretised with very coarse, coarse, medium, fine and very fine meshes. The slope parameters remain the same. The results for slope stability analyses with and without the load are demonstrated in Fig.6 and Fig.7, respectively. It shows coarse meshes result in a slightly high factor of safety and blurred slip surfaces. However, the influence of mesh density on the factor of safety is quite limited. *FS*=1.82 and 1.75 for slopes with very coarse and fine meshes, respectively. For slopes with the distributed load, *FS* =1.48 and 1.44 to

very coarse and fine meshes, respectively. Furthermore, to ensure the reliability of numerical results, over 50 000 elements are normally employed in the following studies.

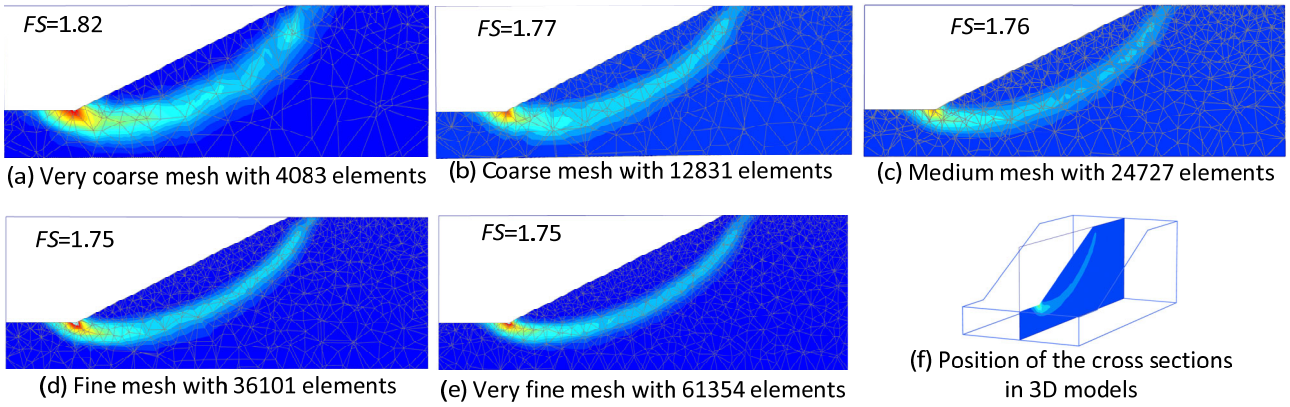


Fig.6. Mesh sensitivity analysis for a slope with *B/H*=2. Colours are proportional to the total deviatoric strain.

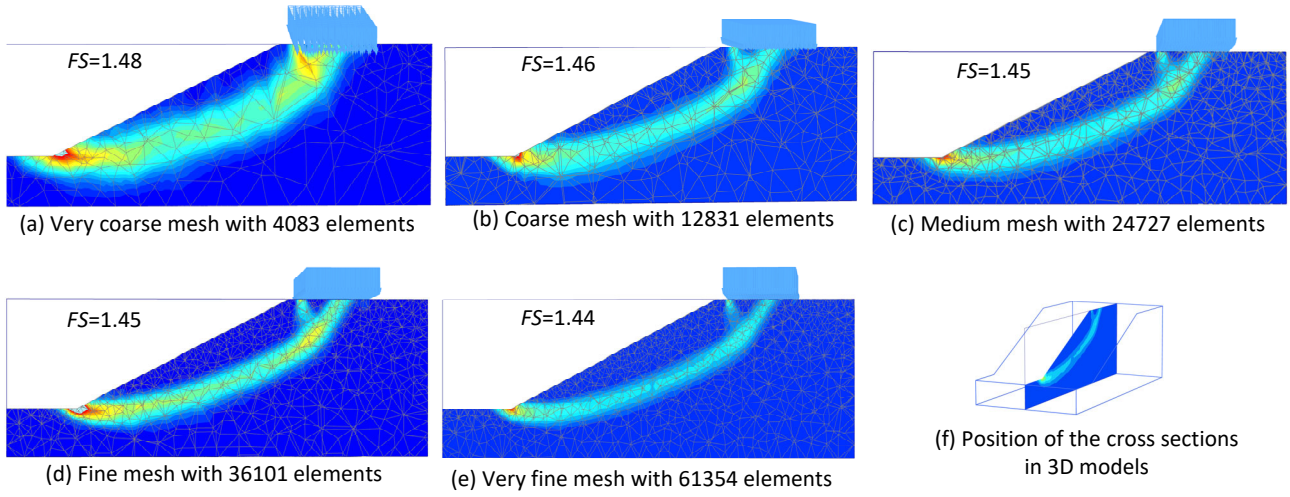


Fig.7. Mesh sensitivity analysis for a slope with a distributed load and *B/H*=2. Colours are proportional to the total deviatoric strain.

3. Charts of three-dimensional effects

As a matter of factor, various factors can affect 3D effects of a slope such as slope geometry and shear strength parameters. Therefore, it is difficult to develop a general analytical solution to this issue. In this study, an empirical approach based on stability charts is used to develop a series of charts on 3D effects. The charts presented below can give a quick reference on 3D effects of a slope. When the 3D effect is significant, a detailed 3D slope stability analysis that can consider complex 3D geometry and boundary condition is advised.

3.1 Purely cohesive slopes

The model geometry of purely cohesive slopes is shown in Fig. 8 involving the slope height H, the slope width B, the slope angle β and the slope depth D.

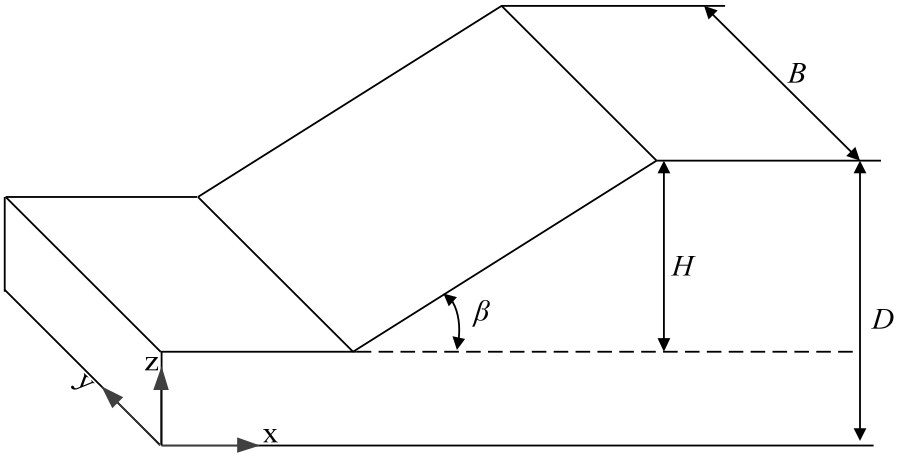


Fig. 8. 3D slope model geometry.

To derive as much data as possible, stability charts in the literature (Li et al., 2009b) are adopted for two- and three-dimensional slope stability analyses under undrained condition. The charts are examined before we are confident to use their data. An idealised slope is used as the first example with the following parameters: β=45°, B=4.5 m, H=4.5 m, D=6 m, unit weight γ=16 kN/m^3 and undrained shear strength c_u=30 kPa. For the second slope, the slope angle β is set to 30° and the slope depth D is changed to 9 m, and the rest of the parameters remain the same. According to the charts,

FS3D is calculated as 3.79 and 4.58, respectively. The numerical results by the finite element strength reduction method for the two slopes show that *FS3D*=3.62 and 4.62, respectively. The difference in the value of *FS3D* determined by the charts and the finite element strength reduction method is very small for the studied slopes. The good agreement between the two methods shows the reliability of the charts. Therefore, the data in the charts can be used to develop the 3D effect charts, in which a ratio of factors of safety *FS3D*/*FS2D* is calculated.

Fig. 9 shows 3D effect charts, in which β is increased from 15˚, 22.5˚, 30˚ to 45˚. The results indicate that the 3D effect is determined by the slope geometric parameters. Material properties such as the unit weight and undrained shear strength do not influence the 3D effect. These findings are also confirmed in the paper (Eid et al., 2006).

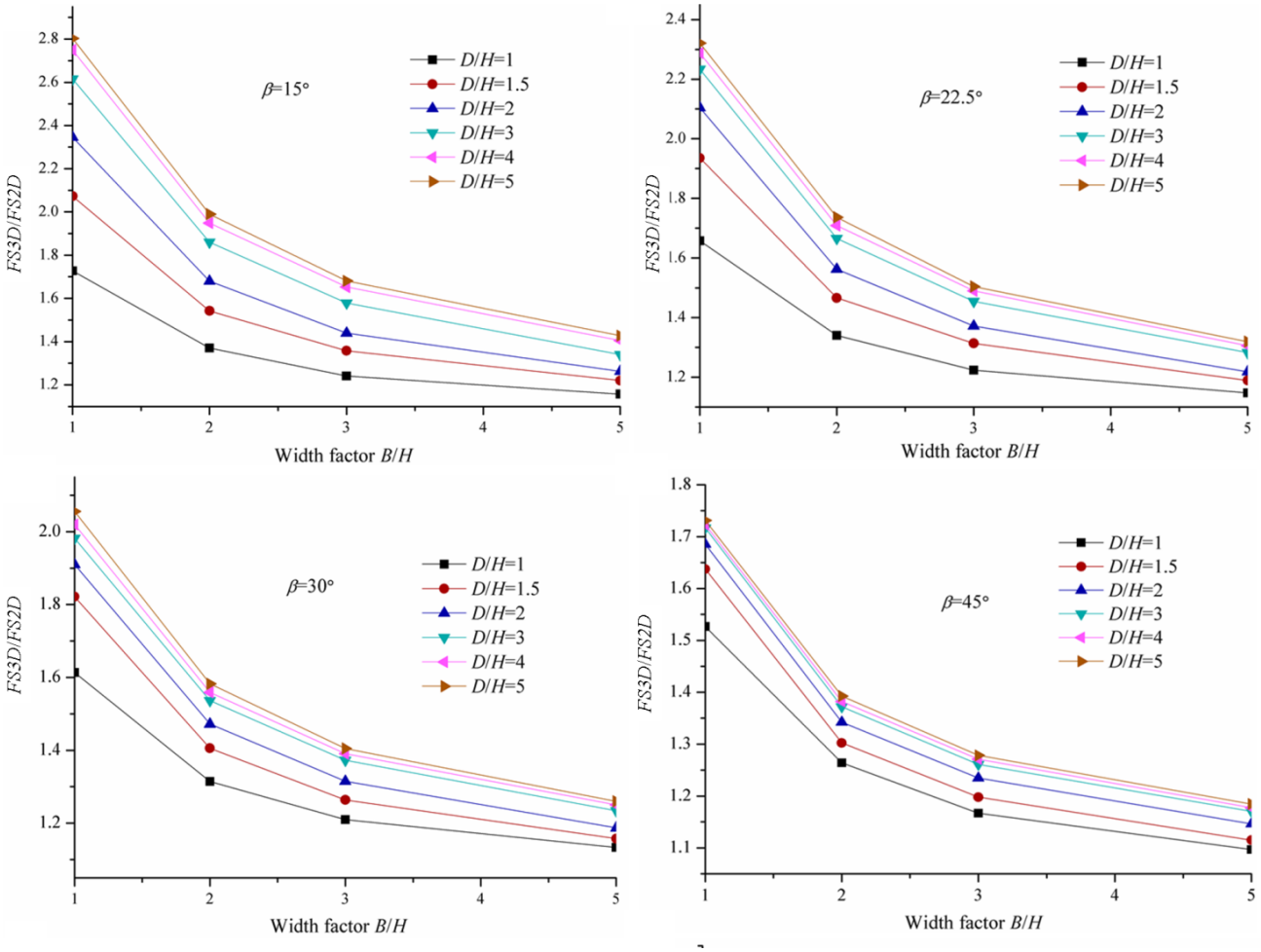


Fig. 9. 3D effect charts for slopes in purely cohesive soils.

3.2 Cohesive-frictional soil slopes

The geometry model of the idealised slope as shown in Fig. 8 is still used in this section. Since the slip surface of cohesive-frictional slopes is relatively shallow, commonly above the slope toe, slope depth D is not required to be treated as an independent variable. The shear strength is determined by effective shear strength parameters where c is the cohesion and φ is the frictional angle. The pore-water pressure conditions are not considered here. The stability charts in (Gao et al., 2013) are adopted in order to obtain more data on slope stability. To examine its accuracy, an example is used with the following parameters β=30˚, H=4.5 m, D=6 m, γ=16 kN/m^3, c=10 kPa and φ=32˚. B/H is increased from 1, 2, 4 to ∞, where B/H=∞ indicates 2D slope stability analysis. Manual estimation from the charts yields FS=3.41, 2.91, 2.75 and 2.59, respectively. The finite element strength reduction approach is also used for these slopes' stability analyses. The numerical results give FS=3.33, 2.92, 2.74 and 2.60, respectively. After the charts are verified, data from the charts and numerical results are collocated and $FS3D/FS2D$ is calculated. Fig. 10 shows 3D effect charts for cohesive-frictional soil slopes.

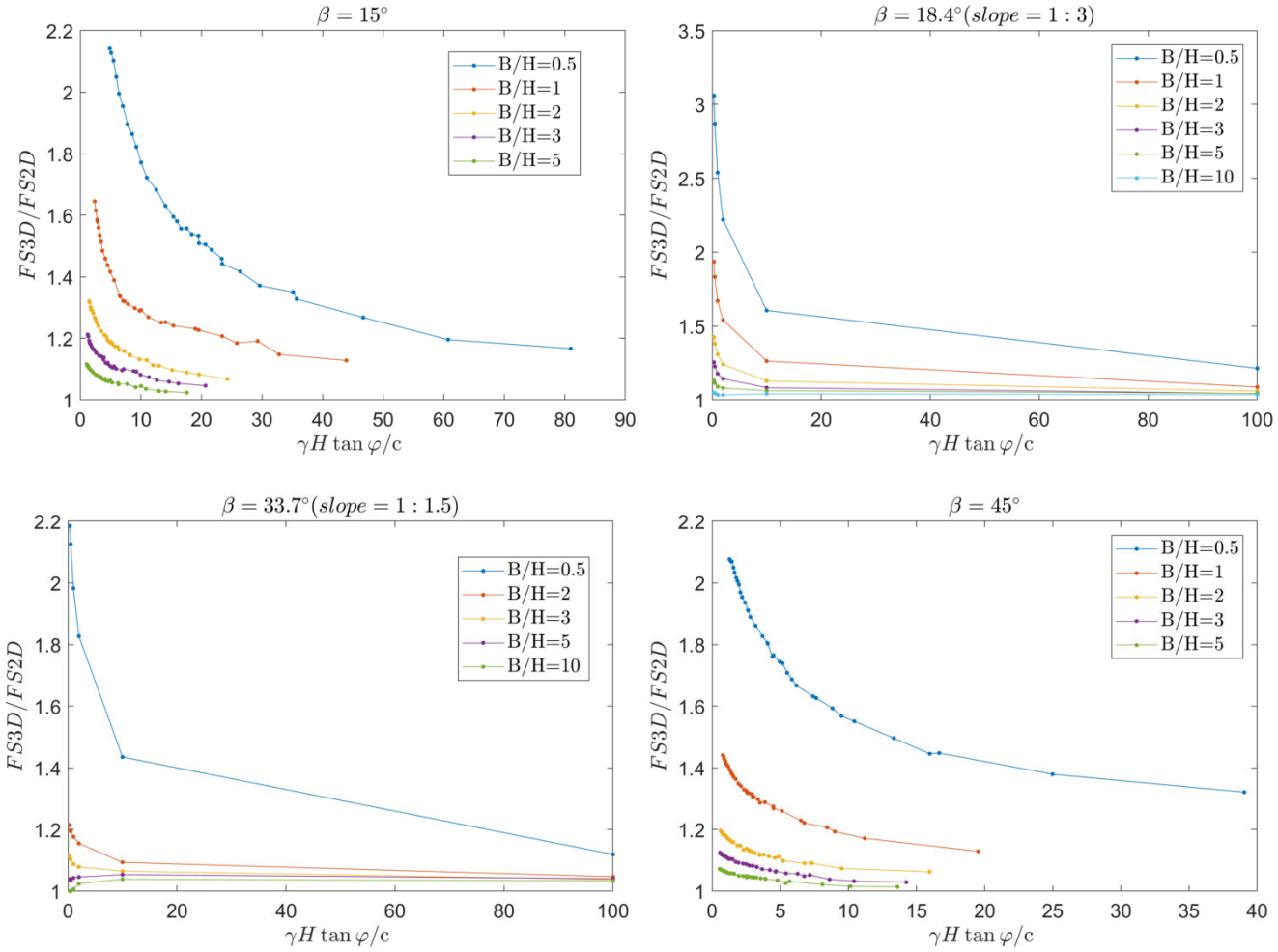


Fig. 10. 3D effect charts for slopes in cohesive-frictional soils. The pore-water pressure conditions are not considered here (dry soil).

In the charts, $\gamma H \tan\varphi / c$ is a dimensionless variable proposed in (Bell, 1966). It is evident that the 3D effect declines with B/H increasing.

3.3 Concave slopes

The design of stable concave slopes with plan curvature such as open-pit mine slopes is of significance in practical engineering. However, to date, few systematic studies have been conducted on stability prediction of concave slopes with a wide range of slope parameters. In this work, the shear strength reduction method with Plaxis 3D (Brinkgreve et al., 2010) and the limit equilibrium method with SLOPE/W (Krahn, 2004) is employed for three- and two-dimensional slope stability analysis.

Fig. 11 shows 3D slope geometry for the defined problem, in which the radius of the plan curvature is denoted by *r*. The typical boundary conditions for a slope stability analysis are adopted. The top surface of the slope is set free, the bottom and side surfaces are fully fixed, and the symmetric surface is fixed in the normal direction. It is necessary to note that for steep slopes that have non-circular slip surfaces, the strength reduction method was used for two-dimensional stability analysis.

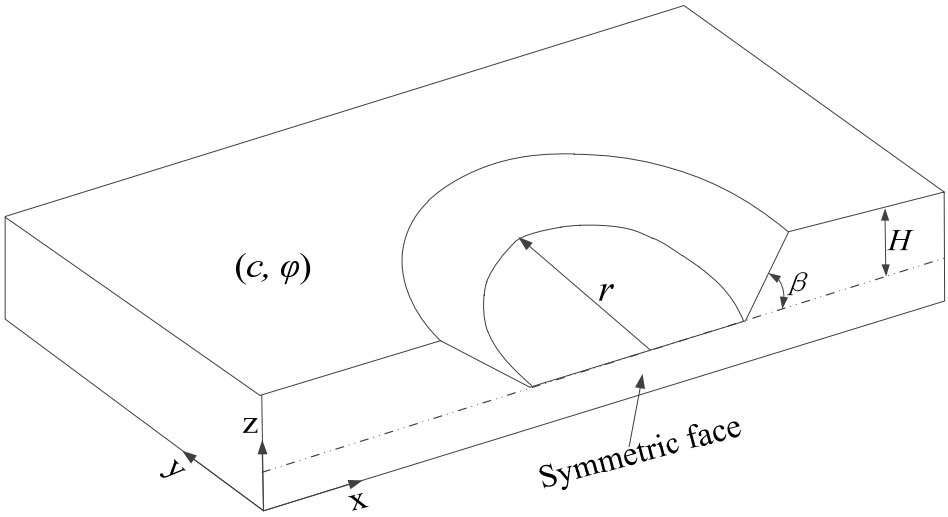


Fig. 11. Model geometry for concave slopes with plan curvature.

Fig. 12 shows two- and three-dimensional numerical results for a concave slope. The failure surfaces can be seen clearly. As concave slopes provide additional confinement for failure mass, a concave slope would possess a higher *FS*.

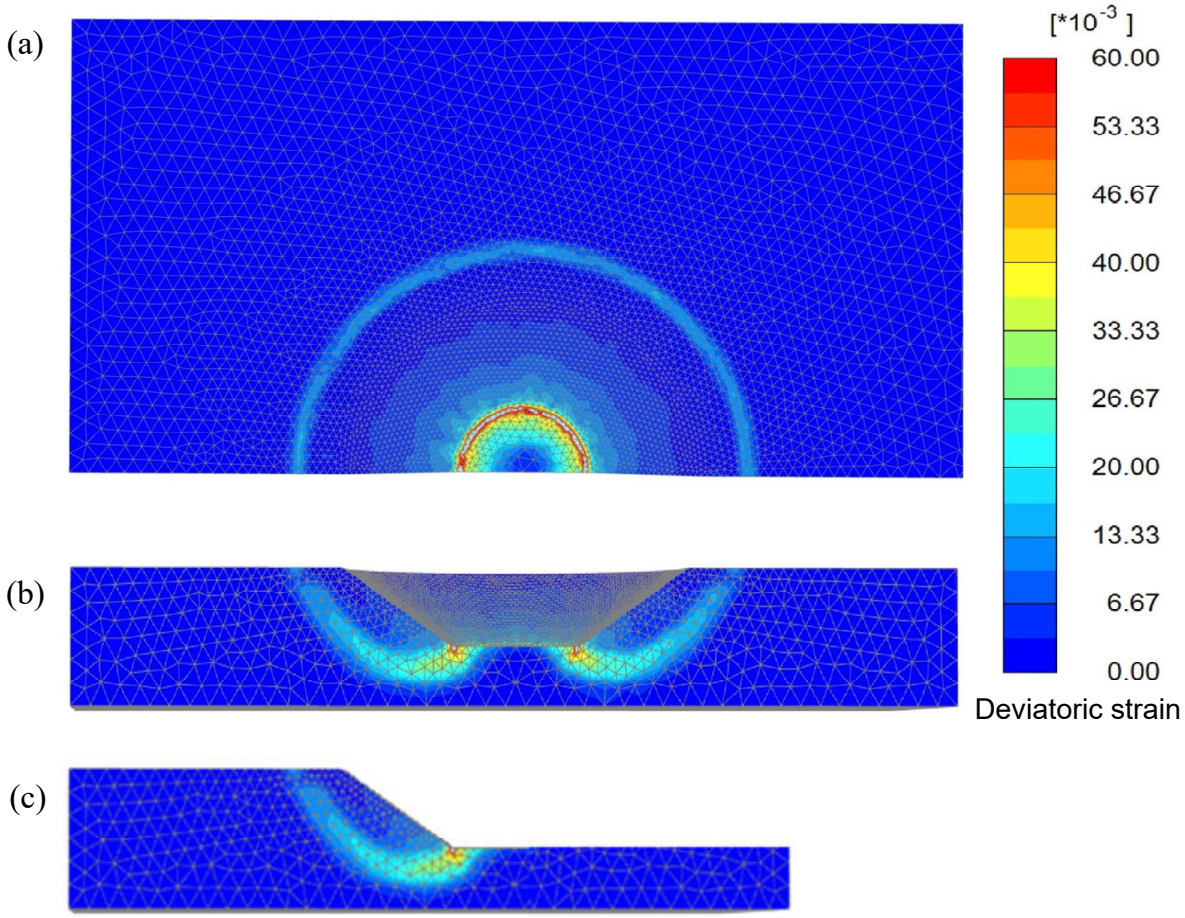


Fig. 12. Failure surface of a concave slope: (a) top view of the 3D analysis results, (b) front view of the 3D analysis results and (c) 2D analysis results. Colours are proportional to the total deviatoric strain.

Based on the numerical results, the stability charts are presented in Fig. 13 for homogeneous concave slopes with plan curvature, in which a wide range of slope angles β, a relative curvature radius r/H, and the dimensionless parameter $c/\gamma H \tan\varphi$ is utilised. It is found that the relative curvature radius has played a key role in 3D effects. Overall, the 3D effect is evident when r/H <1.

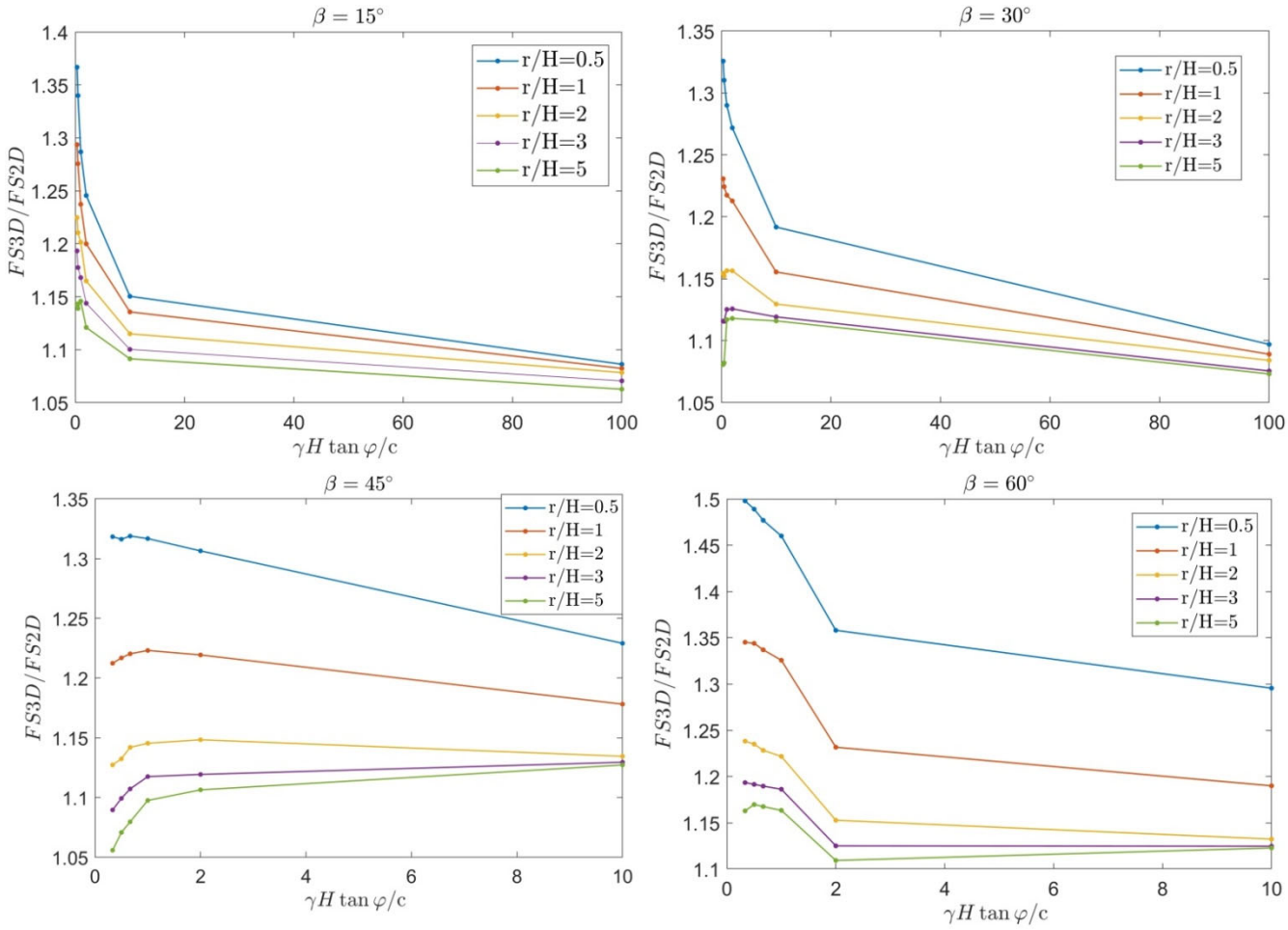


Fig. 13. 3D effect charts for concave slopes in cohesive-frictional soil. The pore-water pressure conditions are not considered here (dry soil).

4. An easy-to-use tool: SlopeLab

To find 3D effects for a slope, users need to determine the most relevant cases in the charts (i.e., Figs. 9, 10 and 13), in which manual estimation is required. For ease of use, a simple tool is developed with a graphical user interface based on the collected data. For this purpose, artificial neural networks (ANN) are used in this work, which functions as a fitting tool. ANN has been used increasingly in the geotechnical engineering community for various challenges (Lee et al., 2003, Das and Basudhar, 2006, Qi et al., 2018, Shahri et al., 2019, Gholami et al., 2020, Lin et al., 2020, Ni et al., 2020, Zhang et al., 2020). The architecture of ANN consists of the input layer, the output layer and several hidden layers, as demonstrated with a typical ANN in Fig. 14. Each layer has several neurons and each neuron typically has weights. The data is processed and transmitted between neurons via connection links (Hassoun, 1995). During the learning process, neurons' weight decreases or increases leading to the varied strength of the signal of that neuron.

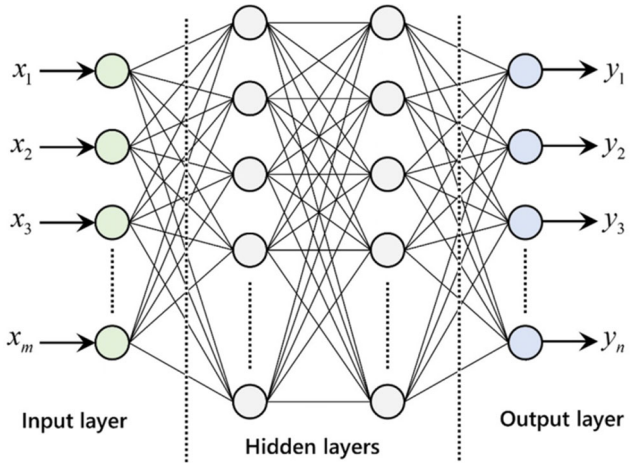


Fig. 14. An ANN architecture with two hidden layers.

A dataset for the ANN is required to be randomly split into two independent subsets: the training dataset and the testing dataset. The ANN is trained with the training data, while the testing dataset is used to verify its predictive performance. In this study, 80% of all the data is used for the training dataset while 20% is used for the testing dataset. The performance of the trained ANN is evaluated with the correlation coefficient R:

$$R = \frac{\sum_{i=1}^{n}\left(C_i - \overline{C}\right)\left(P_i - \overline{P}\right)}{\sqrt{\sum_{i=1}^{n}\left(C_i - \overline{C}\right)^2}\sqrt{\sum_{i=1}^{n}\left(P_i - \overline{P}\right)^2}} \tag{1}$$

where C is measured solutions, P is predicted results, n is the size of the dataset and $\overline{C}$ and $\overline{P}$ are the mean value of the variables. R is a measure of the linear relationship between two variables. A value of 1 indicates a perfect positive correlation while 0 represents that there is no linear correlation between the variables.

After the ANN is trained, its performance is evaluated with the correlation coefficient R. For example, Fig. 15 shows the performance of trained ANN dedicated to the concave slopes. A great performance of the trained neural networks is concluded as the value of R is found being very close to 1. Predicted results agree well with the calculated data.

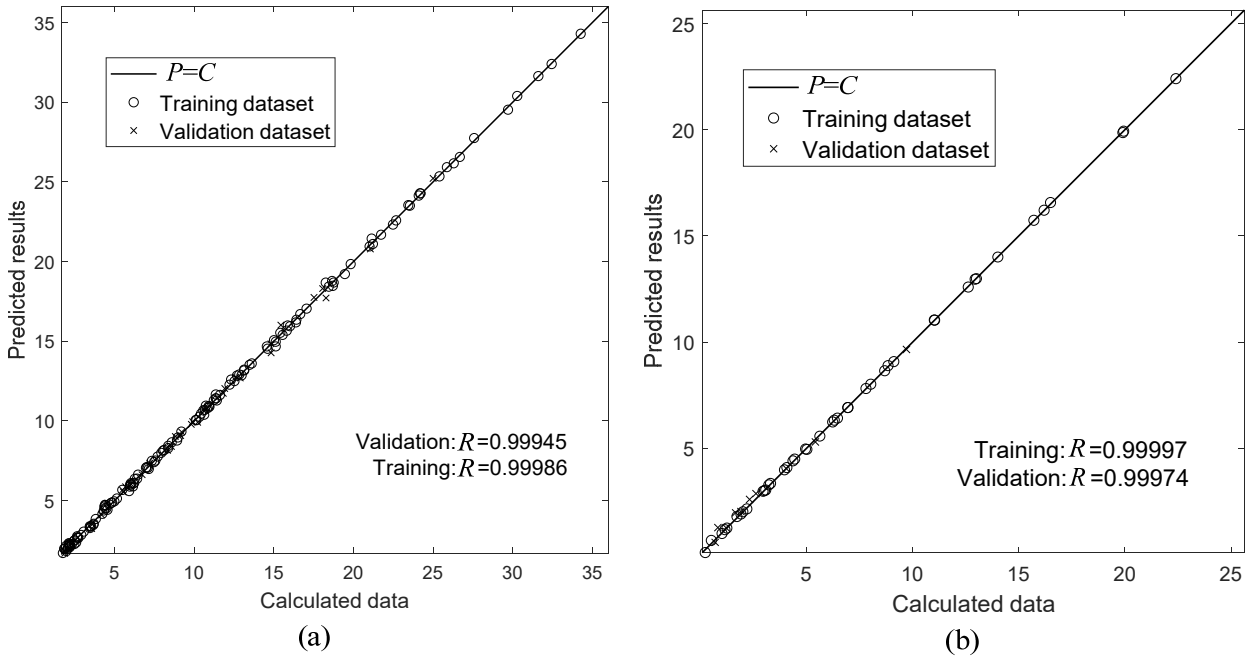


Fig. 15. Performance of the trained ANN dedicated to stability analyses of concave slopes in cohesive-frictional soil: (a) 3D slope stability analysis and (b) 2D slope stability analysis. The pore-water pressure conditions are not considered (dry soil).

5. Application examples

In this section, a series of examples are employed to demonstrate how the stability charts can be used. In addition, the usage of the proposed program will be illustrated, in which parameters can be set. The results from the program will be compared with results from the charts and numerical calculations, showing that the proposed program can provide satisfying results.

5.1. Example 1: an undrained slope

The first example taken from (Griffiths and Marquez, 2007) is a slope in 'undrained clay' with γ=16 kN/m^3, c_u =14.4 kPa and β=26.57˚ (1:2 slope) whose geometry parameters B/H=4 and D/H=1.5. A stability analysis using the finite element strength reduction method has been conducted for this slope yielding *FS3D*=1.45 and 2D limit equilibrium analysis gives *FS2D*=1.25. Therefore, 3D effects for this slope can be measured with *FS3D*/ *FS2D* =1.16.

Fig. 9 provides 3D stability charts for slopes under undrained conditions and a manual procedure is required to reach a solution, as explained below. The chart is presented based on slope cases of B/H=1, 2, 3, 5 and β=7.5˚, 15˚, 22.5˚, 30˚, 45˚, 60˚ and 75˚, the data to the slope with B/H=4 and β=26.57˚ cannot be found straightforwardly. The four closest cases are determined as listed in Table 1, and associated *FS3D*/ *FS2D* is calculated. The results turn out *FS3D*/ *FS2D* of the slope is between 1.16 and 1.31. Finally, linear interpolation of the four numbers gives an estimated value *FS3D*/ *FS2D* =1.23. Therefore, the stability of this slope is underestimated by the 2D solution by greater than 20 % according to the chart solution.

Table 1. Chart solutions of the undrained slope

	β=22.5˚	β=30˚
FS3D/ *FS2D* (*B*/*H*=3)	1.31	1.26
FS3D/ *FS2D* (*B*/*H*=5)	1.19	1.16
Estimated *FS3D*/ *FS2D:* 1.23 (*B*/*H*=4 and β=26.57˚)		

In contrast, the proposed program's usage is very straightforward. For undrained slopes, the value of cohesion is equal to the undrained shear strength and a zero frictional angle is used. The default slope geometry is straight slopes with the plan curvature radius *r* being infinite. After setting the parameters of the slope, two- and three-dimensional factors of safety of the slope are obtained immediately. The result reads *FS3D*=1.63, which agree well with the numerical results. In addition, *FS3D*/*FS2D*=1.29.

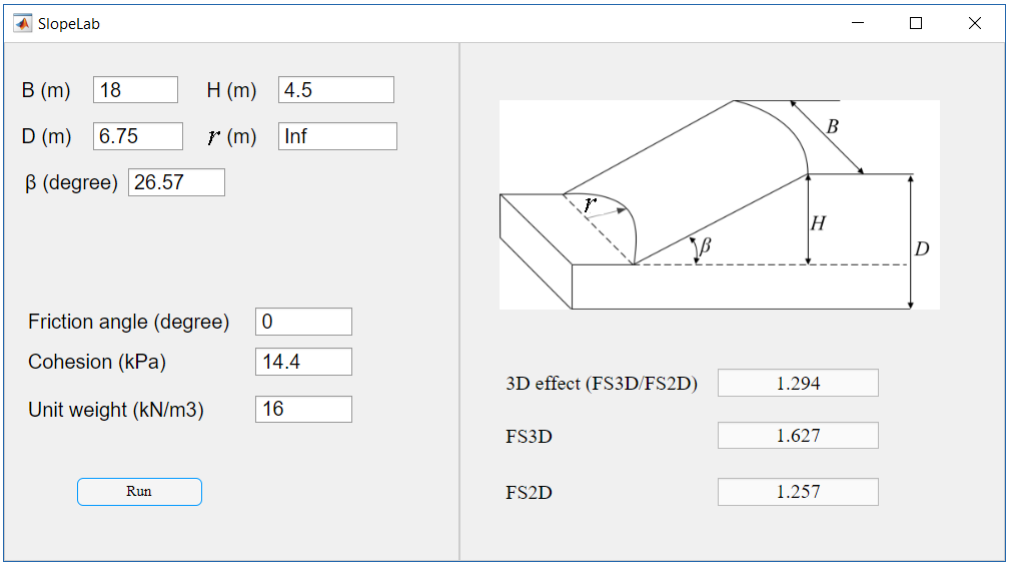


Fig. 16 Results for the undrained slope by the proposed program.

5.2. Example 2: a cohesive-frictional soil slope

The second example considers a homogeneous slope in cohesive-frictional soil. For the slope model, γ=18 kN/m^3, c=4 kPa, φ=31˚, β=37˚ and B/H=1.5. The stability analysis using the finite element strength reduction method is conducted for this slope yielding *FS3D*=1.75 and 2D limit equilibrium analysis gives *FS2D*=1.52, as shown in Fig. 17.

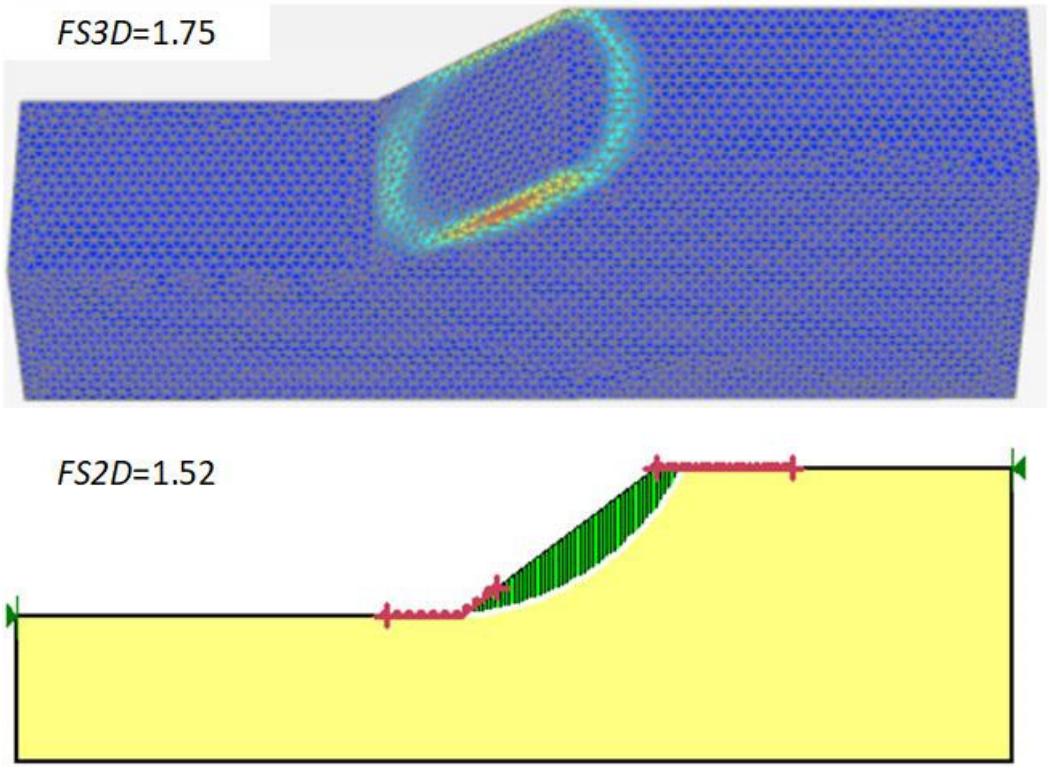


Fig. 17 Calculation results for the slope in cohesive-frictional soil. For finite element numerical results, colours are proportional to the total deviatoric strain.

Fig. 10 provides 3D stability charts based on B/H=0.5, 1.0, 2.0, 3.0, 5.0 and β=15˚, 18.4˚, 33.7˚and 45˚. As a result, the slope with B/H=1.5 and β=37˚ cannot be found in the charts straightforwardly. The four closest cases are determined as listed in Table 2 and associated *FS3D*/ *FS2D* is calculated. The results turn out *FS3D*/ *FS2D* of the slope is between 1.05 and 1.21. Finally, linear interpolation of the four numbers gives an estimated value *FS3D*/ *FS2D* =1.14.

Table 2. Chart solutions of the cohesive-frictional slope

	β=33.7˚	β=45˚
FS3D/ FS2D (*B*/*H*=1)	1.21	1.15
FS3D/ FS2D (*B*/*H*=2)	1.10	1.05
Estimated *FS3D/ FS2D:* 1.14 (*B*/*H*=1.5 and β=37˚)		

After setting the slope's parameters in the program, Fig.18 shows the program's results: *FS3D*=1.69 and *FS2D*=1.53. *FS3D/ FS2D*=1.11. These results are in a very good agreement with the numerical results and chart solutions.

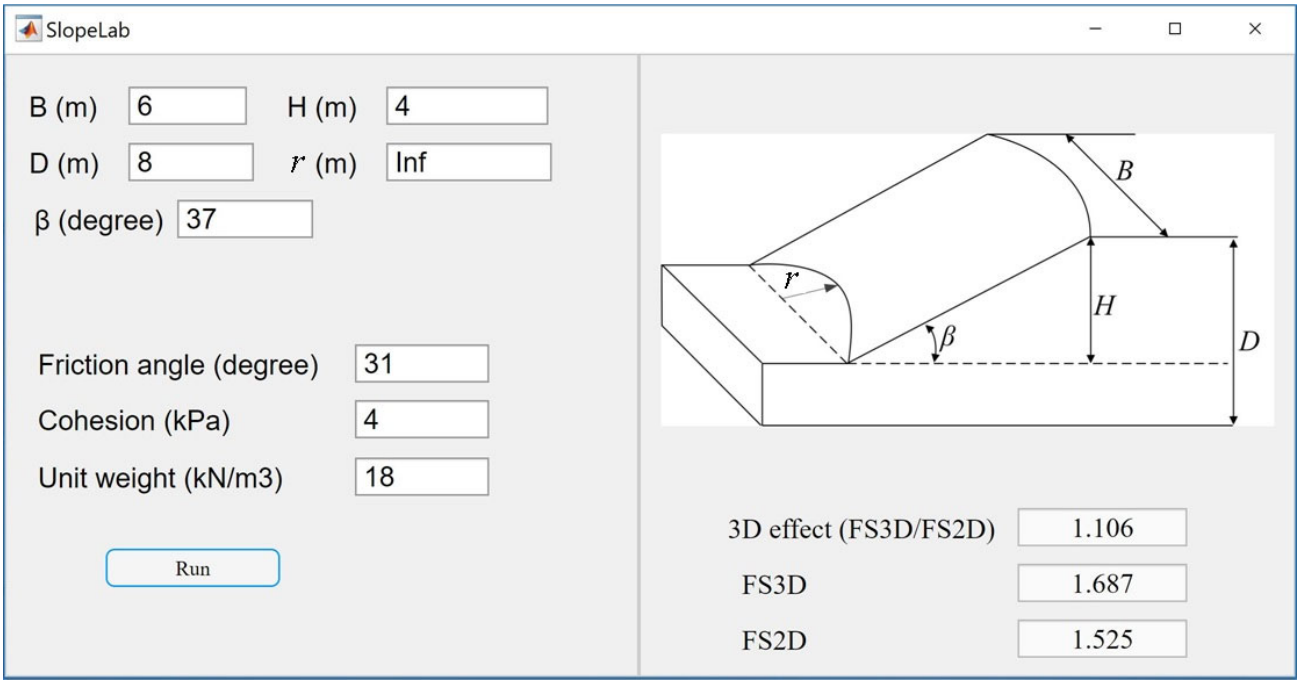


Fig. 18. Results for the cohesive-frictional slope by the proposed program.

5.3. Example 3: a concave slope

The third example involves a homogenous concave slope with γ=18 kN/m^3, c=8 kPa, φ=29˚, β=60˚, H= 4 m and r=2.8 m. The relative curvature of this slope r/H=0.7 whereas available charts are presented based on r/H=0.5, 1, 2, 3 and 5. Following the chart solutions' procedure as described above, *FS3D*/*FS2D* is found as 1.31 and 1.20 for the slopes with r/H=0.5 and r/H=1, respectively. The approximated ratio of factors of safety is *FS3D*/*FS2D* =1.27 for the studied slope. Fig. 19 shows results from the proposed program showing that is *FS3D*/*FS2D* =1.23. A satisfying agreement between chart solution and predicted results by the program has been achieved.

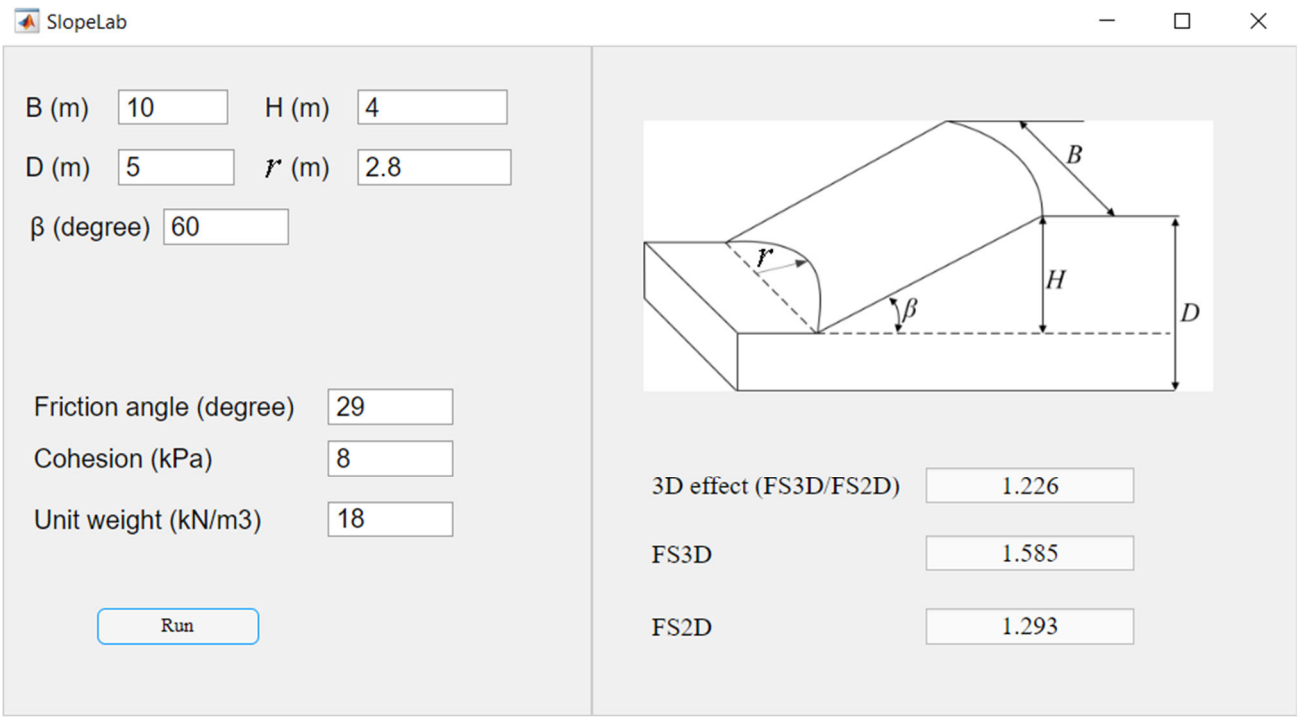


Fig. 19. Results for the concave slope by the proposed program.

Conclusions and discussions

In this work, 3D effects on slope stability calculation are investigated. The 3D effect is measured with a ratio of the safety factor, *FS3D*/*FS2D*. A series of charts on 3D effects have been proposed for slopes under drained and undrained conditions. In addition to the straight slopes, the three-dimensional stability assessment of concave slopes is conducted. A radius is used to define the slope surface' curvature in the horizontal plane. The Mohr-Coulomb failure criterion is used for describing soils' shear strength. Based on the charts, a preliminary estimation on 3D effects for a slope can be estimated. The results can help users to decide if a 2D solution is justifiable for a slope stability analysis. When the 3D effect is significant, a detailed 3D slope stability analysis that can consider complex 3D geometry and boundary condition is advised. In addition, engineers can also understand the impact of slope parameters on 3D effects from the charts.

Overall, *FS3D*/*FS2D* can be larger than 1.4 for undrained uniform slopes when $B/H<=2$. For cohesive-frictional soil slopes, *FS3D*/*FS2D* depends on soil properties. Its value is normally larger than 1.2 when $B/H<=1$. The 3D effect is obvious for 3D concave slopes with plan curvature when $r/H<1$. Therefore, the 3D effect should be considered for slope design in practice, which can avoid unnecessary slope reinforcements.

For ease of use, a digital tool, SlopeLab is developed based on the data in charts and a mathematical model, artificial neural networks. Manually procedures that are required to find closest curves and slope cases when using charts are avoided with the computer program. The performance of the trained artificial neural networks has been evaluated with the correlation coefficient and a series of examples has been employed to show how it can be used.

To address the 3D effect in practice, the following three steps are recommended: (1 a conventional 2D slope stability analysis, (2 a simple 3D slope stability analysis to estimate how large the 3D effect is for the slope and (3 a fully detailed 3D slope stability analysis if the 3D effect cannot be ignored. The second step plays a critical role in these procedures. From the authors' point of view, the proposed charts and the computer program, SlopeLab can be developed to serve a good purpose.

The pore-water pressure conditions are not considered in this work. For future studies, this factor can be taken into account with an additional factor, the pore-water pressure coefficient representing a simplified average pore-water condition in a slope stability analysis. The slopes in this study are assumed to be homogenous and constant Mohr-Coulomb shear strength parameters are used. In addition, many factors such as soil nonhomogeneity, anisotropy, mobilised shear strength, weathering, suction, vegetation, creep deformation, seepage flow and seismic force play a role in slope stability. It would be very difficult to consider these factors with the proposed simplified 3D slope stability analysis framework. When the effect of these factors is necessary to consider, a fully detailed 3D slope stability analysis with dedicated constitutive models is advised.

References

[1] Bell, J. M. 1966. "Dimensionless parameters for homogeneous earth slopes." *J. Soil Mech. Found. Div., Am. Soc. Civ. Eng* 92(5): 51-65.

[2] Bishop, A. W. and Morgenstern, N. 1960. "Stability coefficients for earth slopes." *Geotechnique* 10(4): 129-153.

[3] Brinkgreve, R., Swolfs, W., Engin, E., Waterman, D., Chesaru, A., Bonnier, P. and Galavi, V. 2010. "PLAXIS 2D 2010." *User manual, Plaxis bv*.

[4] Cheng, H. and Zhou, X. 2015. "A novel displacement-based rigorous limit equilibrium method for three-dimensional landslide stability analysis." *Canadian Geotechnical Journal* 52(12): 2055-2066.

[5] Chugh, A. K. 2003. "On the boundary conditions in slope stability analysis." *International journal for numerical and analytical methods in geomechanics* 27(11): 905-926.

[6] Das, S. K. and Basudhar, P. K. 2006. "Undrained lateral load capacity of piles in clay using artificial neural network." *Computers and Geotechnics* 33(8): 454-459.

[7] Dong-ping, D., Liang, L. and Lian-Heng, Z. 2017. "LEM for stability analysis of 3D slopes with general-shaped slip surfaces." *International Journal of Geomechanics* 17(10): 06017017.

[8] Drescher, A. and Michalowski, R. 2009. "Three-dimensional stability of slopes and excavations." *Géotechnique* 59(10): 839-850.

[9] Eid, H. T., Elleboudy, A. M., Elmarsafawi, H. G. and Salama, A. G. 2006. "Stability analysis and charts for slopes susceptible to translational failure." *Canadian geotechnical journal* 43(12): 1374-1388.

[10] Gao, Y., Zhang, F., Lei, G., Li, D., Wu, Y. and Zhang, N. 2013. "Stability charts for 3D failures of homogeneous slopes." *Journal of Geotechnical and Geoenvironmental Engineering* 139(9): 1528-1538.

[11] Gholami, V., Sahour, H. and Amri, M. A. H. 2020. "Soil erosion modeling using erosion pins and artificial neural networks." *Catena* 196: 104902.

[12] Griffiths, D. and Marquez, R. 2007. "Three-dimensional slope stability analysis by elasto-plastic finite elements." *Geotechnique* 57(6): 537-546.

[13] Hassoun, M. H. 1995. Fundamentals of artificial neural networks, *MIT press*.

[14] Hicks, M. A. and Li, Y. 2018. "Influence of length effect on embankment slope reliability in 3D." *International Journal for Numerical and Analytical Methods in Geomechanics* 42(7): 891-915.

[15] Jiang, Q. and Zhou, C. 2017. "A rigorous method for three-dimensional asymmetrical slope stability analysis." *Canadian Geotechnical Journal* 55(4): 495-513.

[16] Kalatehjari, R., Arefnia, A., A Rashid, A. S., Ali, N. and Hajihassani, M. 2015. "Determination of three-dimensional shape of failure in soil slopes." *Canadian Geotechnical Journal* 52(9): 1283-1301.

[17] Krahn, J. 2004. "Stability modeling with SLOPE/W." *An Engineering Methodology: First Edition, Revision* 1: 396.

[18] Lee, S., Lee, S. R. and Kim, Y. 2003. "An approach to estimate unsaturated shear strength using artificial neural network and hyperbolic formulation." *Computers and Geotechnics* 30(6): 489-503.

[19] Leroueil, S. 2001. "Natural slopes and cuts: movement and failure mechanisms." *Geotechnique* 51(3): 197-243.

[20] Leshchinsky, D. and Baker, R. 1986. "Three-dimensional slope stability: end effects." *Soils and Foundations* 26(4): 98-110.

[21] Li, A.-J., Lyamin, A. and Merifield, R. 2009a. "Seismic rock slope stability charts based on limit analysis methods." *Computers and Geotechnics* 36(1-2): 135-148.

[22] Li, A.-J., Merifield, R. and Lyamin, A. 2009b. "Limit analysis solutions for three dimensional undrained slopes." *Computers and Geotechnics* 36(8): 1330-1351.

[23] Lim, K., Lyamin, A., Cassidy, M. J. and Li, A.-J. 2016. "Three-dimensional slope stability charts for frictional fill materials placed on purely cohesive clay." *International Journal of Geomechanics* 16(2): 04015042.

[24] Lin, P., Ni, P., Guo, C. and Mei, G. 2020. "Mapping soil nail loads using Federal Highway Administration (FHWA) simplified models and artificial neural network technique." *Canadian Geotechnical Journal* 57(10): 1453-1471.

[25] Lu, K. L. and Zhu, D. Y. 2016. "A three-dimensional rigorous method for stability analysis and its application." *Bulletin of Engineering Geology and the Environment* 75(4): 1445-1457.

[26] Michalowski, R. L. 2010. "Limit analysis and stability charts for 3D slope failures." *Journal of Geotechnical and Geoenvironmental Engineering* 136(4): 583-593.

[27] Ni, L., Zhang, X., Zou, L. and Huang, J. 2020. "Phase-field modeling of hydraulic fracture network propagation in poroelastic rocks." *Computational Geosciences* 24(5): 1767-1782.

[28] Pandit, K., Sarkar, S. and Sharma, M. 2019. Optimization techniques in slope stability analysis methods. *Landslides: Theory, Practice and Modelling*, Springer**:** 227-264.

[29] Park, D. and Michalowski, R. L. 2017. "Three-dimensional stability analysis of slopes in hard soil/soft rock with tensile strength cut-off." *Engineering geology* 229: 73-84.

[30] Park, D. and Michalowski, R. L. 2018. "Intricacies in three‐dimensional limit analysis of earth slopes." *International Journal for Numerical and Analytical Methods in Geomechanics* 42(17): 2109-2129.

[31] Qi, C., Fourie, A. and Chen, Q. 2018. "Neural network and particle swarm optimization for predicting the unconfined compressive strength of cemented paste backfill." *Construction and Building Materials* 159: 473-478.

[32] Qian, Z., Li, A., Merifield, R. and Lyamin, A. 2015. "Slope stability charts for two-layered purely cohesive soils based on finite-element limit analysis methods." *International Journal of Geomechanics* 15(3): 06014022.

[33] Shahri, A. A., Spross, J., Johansson, F. and Larsson, S. 2019. "Landslide susceptibility hazard map in southwest Sweden using artificial neural network." *Catena* 183: 104225.

[34] Shen, J. and Karakus, M. 2013. "Three-dimensional numerical analysis for rock slope stability using shear strength reduction method." *Canadian geotechnical journal* 51(2): 164-172.

[35] Sloan, S. 2013. "Geotechnical stability analysis." *Géotechnique* 63(7): 531-571.

[36] Sun, C., Chai, J., Xu, Z. and Qin, Y. 2017. "3D stability charts for convex and concave slopes in plan view with homogeneous soil based on the strength-reduction method." *International Journal of Geomechanics* 17(5): 06016034.

[37] Taylor, D. W. 1937. "Stability of earth slopes." *J. Boston Soc. Civil Engineers* 24(3): 197-247.

[38] Troncone, A., Conte, E. and Donato, A. 2014. "Two and three-dimensional numerical analysis of the progressive failure that occurred in an excavation-induced landslide." *Engineering geology* 183: 265-275.

[39] Utili, S. 2013. "Investigation by limit analysis on the stability of slopes with cracks." *Geotechnique* 63(2): 140-154.

[40] Yang, X. and Li, Z. 2018. "Comparison of factors of safety using a 3D failure mechanism with kinematic approach." *International Journal of Geomechanics* 18(9): 04018107.

[41] Zhang, F., Leshchinsky, D., Gao, Y. and Yang, S. 2018. "Three-dimensional slope stability analysis of convex turning corners." *Journal of Geotechnical and Geoenvironmental Engineering* 144(6): 06018003.

[42] Zhang, L., Fredlund, M. D., Fredlund, D. G., Lu, H. and Wilson, G. 2015. "The influence of the unsaturated soil zone on 2-D and 3-D slope stability analyses." *Engineering geology* 193: 374-383.

[43] Zhang, X., Nguyen, H., Bui, X.-N., Le, H. A., Nguyen-Thoi, T., Moayedi, H. and Mahesh, V. 2020. "Evaluating and predicting the stability of roadways in tunnelling and underground space using artificial neural network-based particle swarm optimization." *Tunnelling and Underground Space Technology* 103: 103517.

[44] Zheng, H. 2012. "A three‐dimensional rigorous method for stability analysis of landslides." *Engineering Geology* 145: 30-40.

BIG – Branschsamverkan i grunden
Forskningsprogram för effektiv och säker grundläggning av vägar och järnvägar

BIG

BIG – Branschsamverkan i grunden - är ett forskningsprogram för effektiv och säker grundläggning av transportsystemets infrastruktur. Programmet etablerades under senhösten 2013, och påbörjade sin verksamhet den 1 januari, 2014.

Målsättningen är att sänka kostnader för byggande och underhåll av transportsystemets infrastruktur genom ett långsiktigt och systematiskt utvecklingsarbete inom geoteknikområdet.

I BIG samverkar Trafikverket, Chalmers tekniska högskola, Luleå tekniska universitet, Kungliga tekniska högskolan och Statens geotekniska institut.

Resultat från BIG projekt publiceras i vetenskapliga artiklar och parternas egna rapportserier. Alternativt så publiceras rapporterna i denna gemensamma BIG rapport serie.

Publicerade rapporter

A2014:03	Deformationer i undergrund – Litteratursammanställning och analys
A2014:07	Grundvattensänkning i morän
A2014:13	Höghastighetsspår i Sverige – på bank
A2014:14	On the fundamental relation between soil creep and cyclic pile-soil response
A2016:05	Modelling deformations below high-speed rail
A2017:07	Dynamic response of transition zone on soft clay
A2017:10	Effects of climate change on slopes in sensitive clay
A2017:14	Changes in undrained shear strength as a function of time under embankments
A2018:03	Three-dimensional effects in slope stability calculations